



Research Article

Congo Red Staining in Digital Pathology: The Streamlined Pipeline for Amyloid Detection Through Congo Red Fluorescence Digital Analysis

Giorgio Cazzaniga^a, Maddalena Maria Bolognesi^a, Matteo Davide Stefania^a,
Francesco Mascadri^a, Albino Eccher^{b,c}, Federico Alberici^{d,e}, Federica Mescia^{d,e},
Andrew Smith^f, Filippo Fraggetta^g, Mattia Rossi^h, Giovanni Gambaro^h, Fabio Pagni^a,
Vincenzo L'Imperio^{a,*}

^a Department of Medicine and Surgery, Pathology, Istituto di Ricovero e Cura a Carattere Scientifico (IRCCS) Fondazione San Gerardo dei Tintori, University of Milano-Bicocca, Monza, Italy; ^b Department of Pathology and Diagnostics, University and Hospital Trust of Verona, Verona, Italy; ^c Department of Medical and Surgical Sciences for Children and Adults, University of Modena and Reggio Emilia, University Hospital of Modena, Modena, Italy; ^d Nephrology Unit, Spedali Civili Hospital, Azienda Socio Sanitaria Territoriale (ASST) Spedali Civili di Brescia, Brescia, Italy; ^e Department of Medical and Surgical Specialties, Radiological Sciences and Public Health, University of Brescia, Brescia, Italy; ^f Department of Medicine and Surgery, Proteomics and Metabolomics Unit, University of Milano-Bicocca, Monza, Italy; ^g Pathology Unit, Azienda Sanitaria Provinciale (ASP) Catania, "Gravina" Hospital, Caltagirone, Italy; ^h Division of Nephrology, Department of Medicine, University of Verona, Verona, Italy

ARTICLE INFO

Article history:

Received 20 July 2023

Revised 4 August 2023

Accepted 21 August 2023

Available online 25 August 2023

Keywords:

amyloidosis

Congo red fluorescence

digital pathology

renal biopsy

ABSTRACT

Renal amyloidosis is a rare condition caused by the progressive accumulation of misfolded proteins within glomeruli, vessels, and interstitium, causing functional decline and requiring prompt treatment due to its significant morbidity and mortality. Congo red (CR) stain on renal biopsy samples is the gold standard for diagnosis, but the need for polarized light is limiting the digitization of this nephropathology field. This study explores the feasibility and reliability of CR fluorescence on virtual slides (CRFVs) in evaluating the diagnostic accuracy and proposing an automated digital pipeline for its assessment. Whole-slide images from 154 renal biopsies with CR were scanned through a Texas red fluorescence filter (NanoZoomer S60, Hamamatsu) at the digital Nephropathology Center of the Istituto di Ricovero e Cura a Carattere Scientifico San Gerardo, Monza, Italy, and evaluated double-blinded for the detection and quantification through the amyloid score and a custom ImageJ pipeline was built to automatically detect amyloid-containing regions. Interobserver agreement for CRFVs was optimal ($k = 0.90$; 95% CI, 0.81–0.98), with even better concordance when consensus-based CRFVs evaluation was compared to the standard CR birefringence (BR) ($k = 0.98$; 95% CI, 0.93–1). Excellent performance was achieved in the assessment of amyloid score overall by CRFVs (weighted $k = 0.70$; 95% CI, 0.08–1), especially within the interstitium (weighted $k = 0.60$; 95% CI, 0.35–0.84), overcoming the misinterpretation of interstitial and capsular collagen BR. The application of an automated digital pathology pipeline (Streamlined Pipeline for Amyloid detection through CR fluorescence Digital Analysis, SPADA) further increased the performance of pathologists, leading to a complete concordance with the standard BR. This study represents an initial step in the validation of CRFVs, demonstrating its general reliability in a digital nephropathology center. The computational method used in this study has the potential to

These authors contributed equally: Giorgio Cazzaniga and Maddalena Maria Bolognesi.

* Corresponding author.

E-mail address: vincenzo.limperio@gmail.com (V. L'Imperio).



facilitate the integration of spatial omics and artificial intelligence tools for the diagnosis of amyloidosis, streamlining its detection process.

© 2023 THE AUTHORS. Published by Elsevier Inc. on behalf of the United States & Canadian Academy of Pathology. This is an open access article under the CC BY-NC-ND license (<http://creativecommons.org/licenses/by-nc-nd/4.0/>).

Introduction

Amyloidosis (AL) is a rare condition characterized by the progressive deposition of misfolded proteins within organs and tissues. Kidneys are often the target of the disease, with proteinuria and deterioration of renal function being the most frequent manifestations, often representing the sentinel of underlying genetic, inflammatory, or neoplastic diseases.¹ For these reasons, its detection is pivotal to promptly initiate the most appropriate treatment and prevent its progression to end-stage renal disease.^{2–4} Even when clinically suspected, renal biopsy remains the gold standard for diagnosis, especially with the use of special histochemical stains. Congo red (CR), which binds to misfolded proteins, is usually used for this purpose, resulting in typical birefringence (BR) under polarized light.⁵ Although it is the most reliable stain in the clinical setting^{6,7} and complements the role of electron microscopy and immunogold labeling,⁸ false-positive and false-negative results have been reported.⁹ In addition, the need for polarized light can significantly complicate the digitization of this technique, slowing down some of the digital transition for these cases.^{10,11} A possible solution to this conundrum is the Congo red fluorescence (CRF) technique, which has already been proposed as a valuable alternative to BR when appropriately standardized using a Texas red fluorescence filter (TRITC).^{12,13} This technique has also been shown to perform better than the “traditional” CR BR.¹⁴ However, no attempt has yet been made to standardize the digitization of CR evaluation by whole-slide imaging (WSI), which may pave the way for the application of computational pathology tools (eg, artificial intelligence)¹⁵ and new in situ proteomics techniques.¹⁶ The present study investigates the feasibility and reliability of CRF on virtual slides (CRFVs) compared to the standard BR in a digital nephropathology center^{10,11} and proposes an automated image analysis pipeline (streamlined pipeline for amyloid detection through Congo red fluorescence digital analysis [SPADA]—Italian for sword, from Latin *spatha*) to further facilitate amyloid detection by the nephropathologist.

Methods and Methods

Cases

The digital archives of the Centre of Nephropathology at Istituto di Ricovero e Cura a Carattere Scientifico Fondazione San Gerardo dei Tintori, University of Milano-Bicocca in Monza, were interrogated from January 2018 to January 2023 to retrieve renal biopsy samples with available CR. For these cases, the final histologic diagnosis, including details of light microscopy, immunofluorescence, and electron microscopy, was retrieved from the Spectrum electronic database (Leica Biosystem).¹⁰ Clinical and laboratory information (sex, age, serum creatinine [milligrams per deciliter], proteinuria [grams per 24 hours], serum/urine M spike, medical history of chronic inflammatory/infectious disease) was recorded and fully annotated. The approval of the local ethics committee was obtained (PNRR-MR1-2022-12375735; March 16, 2023).

Digital Pathology and Automated Image Analysis Pipeline

Renal biopsy slides stained with CR were digitized and WSIs were acquired with a digital slide scanner (NanoZoomer S60, Hamamatsu) at 20× magnification in 2 fluorescence filter combinations:

1. Texas red filter—TRITC—(556/20 excitation—617/73 emission).
2. A scramble filter combination to detect autofluorescence in tissue (480/17 excitation—617/73 emission).

To assess the comparability and reliability of CRFVs and BR, the obtained WSIs were blindly evaluated by 2 nephropathologists (V.L. and F.P.) to assess the presence/absence of amyloid deposits. The results obtained from the virtual slides were then compared between the 2 pathologists and, after resolving discrepancies by consensus, with the actual diagnoses of the renal biopsies to determine the concordance and reliability of the assessments. Furthermore, the positive slides were scored with both methods using the validated amyloid score (AS),¹⁷ which is a scoring system for assessing the severity of amyloid deposition in tissue, to further investigate concordance between observers and CRFVs. The AS is based on the distribution and quantitative involvement of different renal compartments as determined by the sum of scores from 0 to 3 for the glomerular mesangium, glomerular capillary walls, interstitium (I), and vessels (V), with total scores ranging from 0 to 12 and with higher scores indicating more severe AL.^{18,19}

Furthermore, an image analysis using ImageJ was performed to eliminate the background autofluorescence, providing the pathologist with an even more effective means of assessing the presence of amyloid deposits.²⁰ An automated workflow (SPADA) was created to run the script automatically on all images, ensuring a consistent and efficient amyloid detection process (Fig. 1).

Statistical Analysis

For continuous variables, mean and SD were calculated, as appropriate, while qualitative variables were reported as count and frequency. For the comparison of means and qualitative variables, the *t* test and χ^2 test were used, as appropriate, considering *P* values <.05 as statistically significant. Of these, renal biopsies were grouped based on the presence/absence of AL and this has been used for subsequent statistical analysis. To evaluate the correlation between the 2 methods and the agreement between the pathologists, concordance rate, sensitivity, specificity, positive predictive value, negative predictive value, and Cohen's kappa coefficient (κ) (for dichotomous variables) were calculated. The weighted kappa coefficient (*Wk*, quadratic function) was used to measure the correlation of each continuous parameter of AS. The corresponding *P* value and the 95% CI were calculated as appropriate. Statistics were extracted using Excel 2016 (Microsoft) and Python libraries including pandas and scikit-learn.

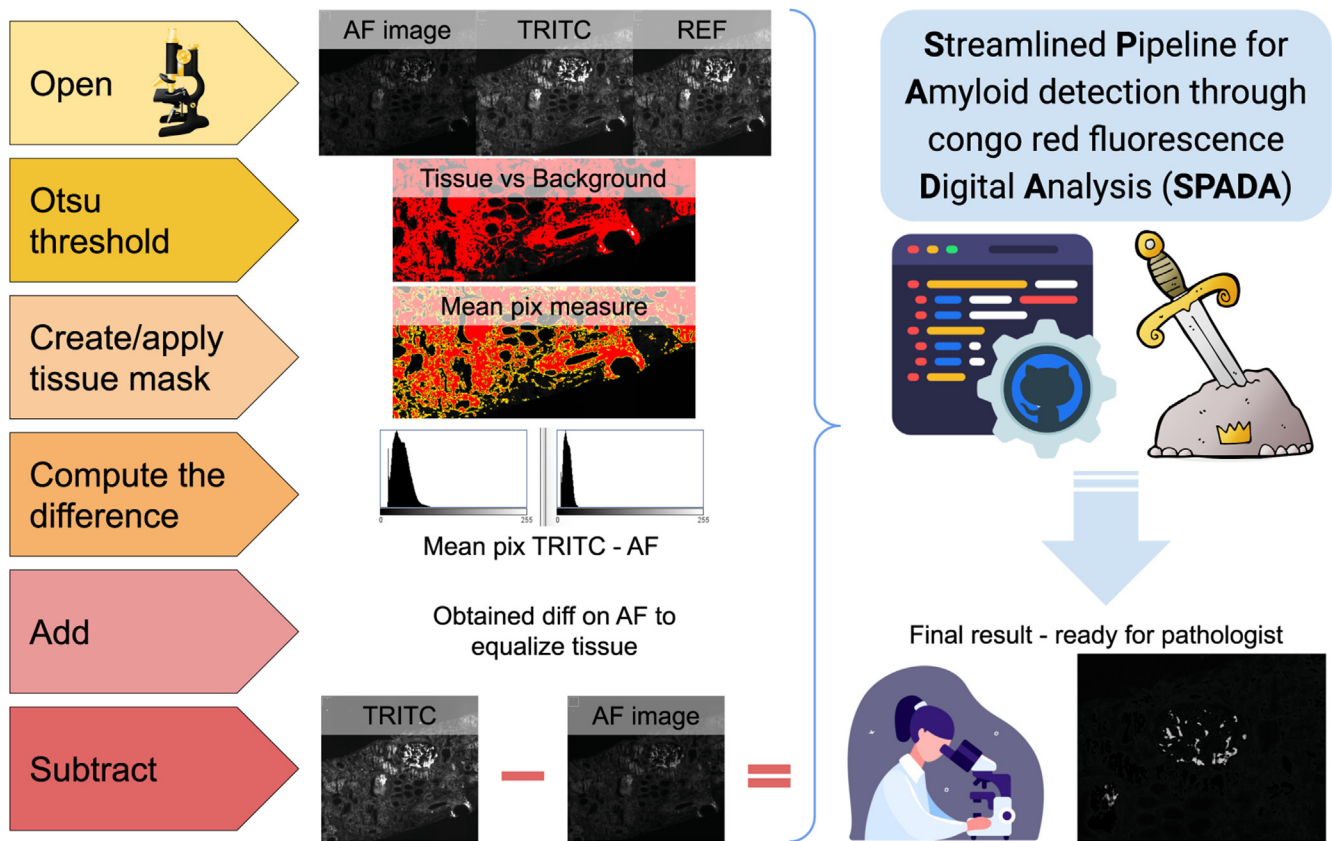


Figure 1.

Workflow of the automated digital pathology pipeline (streamlined pipeline for amyloid detection through Congo red fluorescence digital analysis [SPADA] tool) for the detection of amyloid deposits on renal biopsy samples through Congo red virtual fluorescence. AF, autofluorescence; diff, difference; REF, reference; TRITC, Texas red fluorescence filter.

Results

Cases

A total of 154 renal biopsy samples with available CR were retrieved and evaluated after digitization under a TRITC filter. Of these, 41 cases presented AL, while the other 113 were affected by 23 different diseases, including 20 cases of focal segmental glomerulosclerosis, 19 cases of minimal change disease, 15 cases of diabetic nephropathy, 12 cases of arterionephrosclerosis, 9 cases of membranous nephropathy, 8 cases of monoclonal immunoglobulin deposition disease, 6 cases of cast nephropathy, and other diseases accounting for less than 4 cases each. Cases of AL were represented mostly by light chain AL, 5 cases of Serum Amyloid A protein-associated (AA) AL (1 associated with primary sclerosing cholangitis, 1 associated with familial Mediterranean fever, and 3 of unknown origin), and 1 non-AA, non-AL case. Results of statistical analysis made on clinical and laboratory information showed that none of the features analyzed reached the statistical significance between the 2 groups, as shown in [Table 1](#).

Congo Red Birefringence vs Congo Red Fluorescence on Virtual Slides

Excellent interobserver agreement was recorded for the blind evaluation of CRFVs with a concordance rate of 0.96 (95% CI, 0.92-0.98) and a Cohen's *k* of 0.90 (95% CI, 0.81-0.98), with 3

false-positive and 3 false-negative cases ([Fig. 2A](#)). Discordant cases were usually characterized by a low amount of amyloid deposits, as determined by the AS (a maximum of 3/12 was given in the misclassified cases), and were solved by consensus among the 2 nephropathologists. After this process, in the overall assessment, 40 cases were considered positive on CRFVs, with 1 case of AA AL misclassified as negative due to a scan artifact that was resolved after a rescans. This analysis showed a sensitivity and negative predictive value of 1 (95% CI, 0.91-1 and 0.97-1, respectively) and specificity and positive predictive values of 0.99 (95% CI, 0.95-1) and 0.98 (95% CI, 0.87-1), respectively ([Fig. 2B](#)).

Amyloid Score Evaluation With Congo Red Birefringence vs Congo Red Fluorescence on Virtual Slides

The evaluation of AS on CRFVs by the 2 nephropathologists showed an overall excellent concordance ($Wk = 0.81$; 95% CI, 0.21-1), with better performances for V and I (Wk of 0.73 [95% CI, 0.50-0.97] and 0.71 [95% CI, 0.50-0.92], respectively; [Fig. 2C](#)). The assessment of AS on CRFVs as compared to the standard BR demonstrated an overall good correlation ($Wk = 0.70$; 95% CI, 0.08-1), with the best performances for the V parameter ($Wk = 0.74$; 95% CI, 0.51-0.98) and the worst for the I one ($Wk = 0.60$; 95% CI, 0.35-0.84; [Fig. 2D](#)). Percentages of cases with higher values of each component of AS for the 2 assessment methods are reported in [Table 2](#) and graphically represented as normalized values in [Figure 3](#), showing statistically significant differences for every parameter.

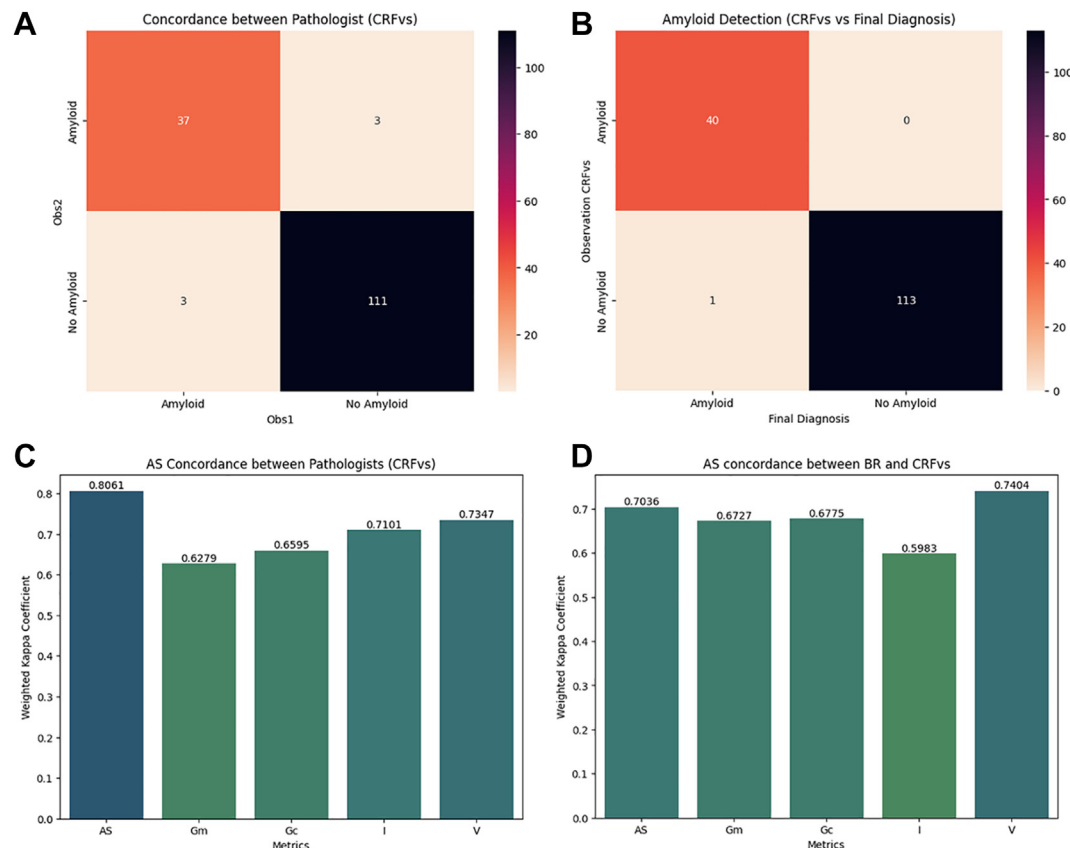
Table 1
Clinical features of the study cohort

| Variables | Other | Amyloidosis | Full cohort | P value |
|--|---------------------------|---------------------------|---------------------------|---------|
| Total cases | 113 | 41 | 154 | |
| Sex, n (%) (95% CI) | | | | |
| Female | 40 (35) (26–44) | 17 (41) (28–57) | 57 (37) (30–45) | 1 |
| Male | 73 (65) (56–74) | 24 (59) (43–72) | 97 (63) (55–70) | |
| Age (y), mean \pm SD (95% CI) | 62 \pm 14.1 (59.4–64.6) | 66 \pm 11.2 (62.6–69.4) | 63 \pm 13.5 (60.9–65.1) | .1 |
| Serum creatinine (mg/dL), mean \pm SD (95% CI) | 2.7 \pm 2.3 (2.2–3.1) | 2.4 \pm 1.7 (1.9–2.9) | 2.6 \pm 2.1 (2.3–2.9) | .6 |
| Proteinuria (g/24 h), mean \pm SD (95% CI) | 4.8 \pm 4.2 (4–5.5) | 5 \pm 2.9 (4.1–5.9) | 4.9 \pm 3.9 (4.6–5.5) | .8 |
| M spike, n (%) (95% CI) | | | | |
| Present | 48 (43) (34–52) | 21 (51) (36–66) | 69 (45) (37–53) | 1 |
| Absent | 63 (57) (47–65) | 20 (49) (34–64) | 83 (54) (46–62) | |

Automated Digital Pathology Pipeline for the Detection of AL

The evaluation of the 154 cases by the 2 nephropathologists highlighted an increased tissue background in the renal biopsy samples scanned with a Texas red filter as compared to the autofluorescence WSI, which could partially account for the few false-negative and false-positive results observed in the study. However, the observation of an average higher pixel value difference between amyloid deposits and normal tissue in CRFVs as compared to the difference between normal tissue in CRFVs and autofluorescence WSI (1.5- to 2-fold higher) suggested as possible

solution the creation of an automated digital pathology pipeline to subtract the noisy background, highlighting specifically the deposits on CRFVs. The application of such computational analysis took an average of 1 minute and 14 seconds per case, with 3 hours and 10 minutes for the script to complete the analysis of the entire data set. The application of such a computation tool allowed to overcome the limitation of BR in highlighting the confounding interstitial/capsular collagen, as demonstrated by the exemplificative case in Figure 3. This efficient computational method (SPADA) allowed for rapid evaluation of the images and facilitated the quantitative assessment of amyloid deposition across the

**Figure 2.**

(A, B) The confusion matrix for comparison of results from 2 different nephropathologists on the same Congo red fluorescence virtual slide (CRFVs) and the consensus results on the CRFVs compared to the final diagnosis of amyloidosis, are shown on birefringence (BR), respectively. (C, D) The histograms show the comparison of weighted kappa coefficients for the different elements that make up amyloid score (AS) as evaluated by the 2 nephropathologists and as assessed on CRFVs and BR, respectively. Gc, glomerular capillary walls; Gm, glomerular mesangium; I, interstitium; Obs, observer; V, vessels.

Table 2

Percentage of cases with higher values of each component of amyloid score for the 2 assessment methods

| Comparisons | AS, n (%) (95% CI) | Gm, n (%) (95% CI) | Gc, n (%) (95% CI) | I, n (%) (95% CI) | V, n (%) (95% CI) |
|-------------|-----------------------|-----------------------|-----------------------|----------------------|----------------------|
| BR > CRFvs | 8 (20) (10–34) | 7 (17) (8–20) | 7 (17) (8–32) | 2 (5) (0.5–17) | 10 (24) (14–40) |
| BR = CRFvs | 14 (34) (22–50) | 23 (56) (41–70) | 22 (54) (39–68) | 30 (73) (58–84) | 23 (56) (41–70) |
| BR < CRFvs | 19 (46) (32–61) | 11 (27) (16–42) | 12 (29) (18–45) | 9 (22) (12–37) | 8 (20) (10–34) |
| P value | <.01 | <.01 | <.01 | <.01 | <.01 |

Statistically significant differences were found in the localization and quantification of amyloid deposits between CRFvs and BR.

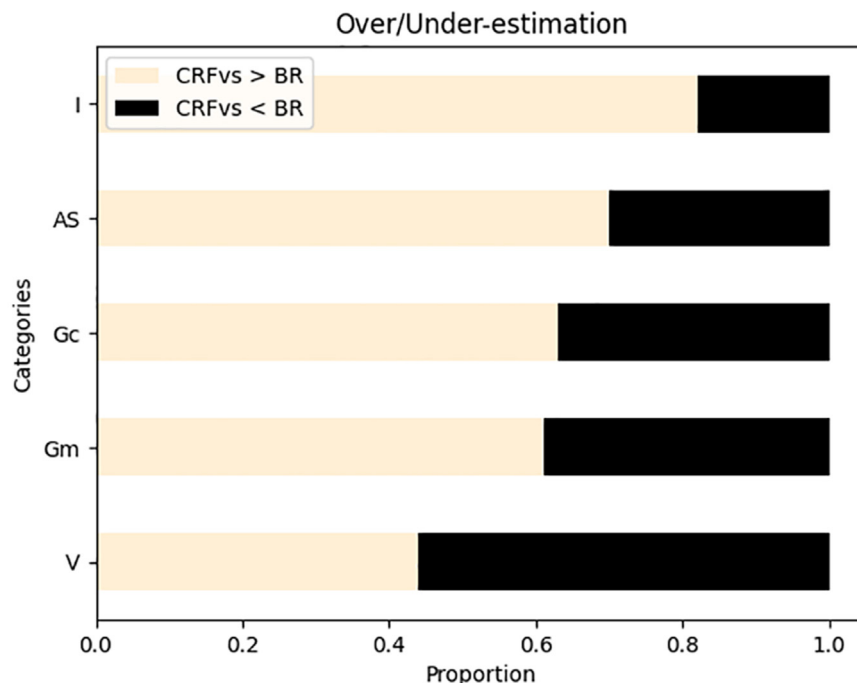
AS, amyloid score; BR, birefringence; CRFvs, Congo red fluorescence virtual slide; Gc, glomerular capillary wall; Gm, glomerular mesangium; I, interstitium; V, vessels.

samples (Fig. 4), leading to a complete concordance with BR when the pipeline was applied by the 2 nephropathologists after a washout period of 2 weeks.

Discussion

The diagnosis of renal AL can be a real challenge, as suspicion often arises in the presence of monoclonal gammopathy of unknown significance (MGUS) or concurrent extrarenal organ dysfunction (eg, congestive heart failure). Attempts have been made to predict amyloid deposition by complex clinical nomograms, with partial success only for localized entities (eg, heart) and specific forms of amyloid (eg, transthyretin),²¹ while no definitive clinical evidence is available for the remaining cases.²² Furthermore, approximately 60% of patients with MGUS who

undergo renal biopsy may have renal disease unrelated to M spikes.²³ This was also demonstrated by the present experience, which shows no significant differences in M spikes between the 2 groups and a variety of alternative diagnoses (eg, minimal change disease, focal segmental glomerulosclerosis, membranous nephropathy, or diabetes) even in the presence of concurrent MGUS. For these reasons, careful assessment of the renal biopsy sample is paramount for the detection of even minute amyloid deposits, highlighting the need for centralization in specialized nephropathology centers through the use of digital pathology infrastructures.^{10,11} In this setting, CR stain needing the examination under polarized light is still a problem for digital transition; even though scanners with polarizable lenses exist, they are not universally accessible, and often they are available only in research contexts.²⁴ Moreover, the limitations associated with the BR nature of amyloid after CR stain further hamper a solid and reliable evaluation of this test, whose “apple green” character is not always obvious²⁵ and other authors list the requirements for its proper and robust assessment (eg, coverslips, mechanical circular stage for slide orientation, and no polarizing filter with a built-in compensator to avoid color and intensity changes).^{26,27} A possible solution to this problem is the evaluation of CRF, first described by Cohen et al²⁸ in 1959 and reliably applicable to a wide range of organs, with optimal performance even in the presence of tiny deposits.^{12,13,29} This has led some authors to propose a reflex test of CRF in cases with negative BR.³⁰ However, no attempt has yet been made to evaluate CRF on WSIs (CRFvs), which can overcome the current intrinsic limitation of CR BR scanning and open the door to the various advantages of slide digitization (eg, sharing, storage, training, and future application of omics and artificial intelligence tools).³¹ Overall, the comparative analysis showed strong agreement between the 2 methods, suggesting that CRFvs assessment could serve as a valid alternative to the standard BR.

**Figure 3.**

Normalized proportion of cases with different values in each element of amyloid score (AS) between Congo red fluorescence virtual slide (CRFvs) and birefringence (BR). The stacked plot illustrates the tendency to achieve higher results with CRFvs on the AS categories and the overall score. Gc, glomerular capillary walls; Gm, glomerular mesangium; I, interstitium; V, vessels.

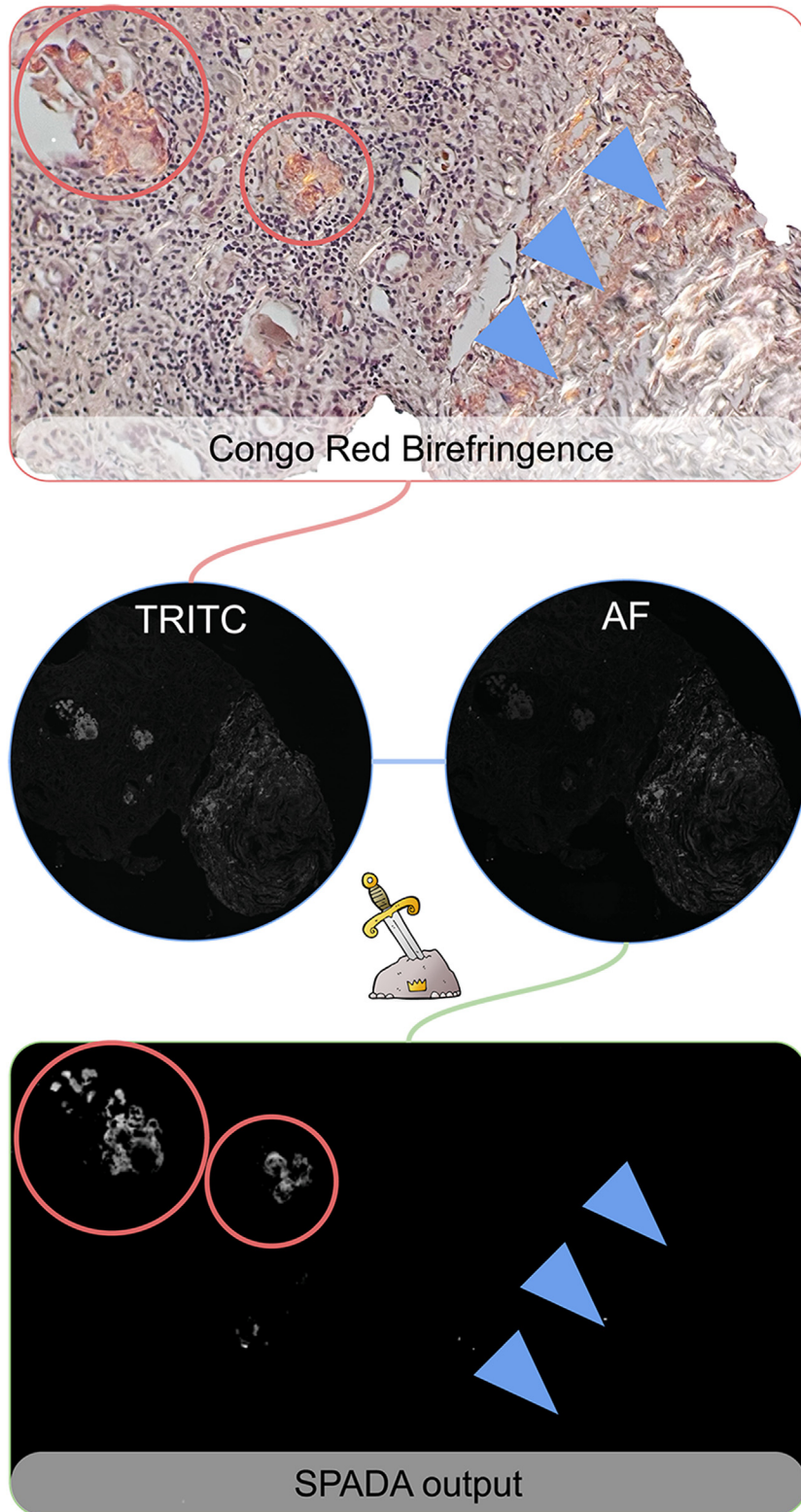


Figure 4.

Exemplary case showing birefringence with Congo Red within the glomeruli (red circles) and peculiar white strong signal under polarized light corresponding to the collagen of the renal capsule (blue arrowheads). The use of the automated pipeline for the detection of amyloid deposits by Congo Red fluorescence (streamlined pipeline for amyloid detection through Congo red fluorescence digital analysis [SPADA] tool) allowed the correct identification of glomerular deposits (red circles) with the complete disappearance of the confounding signal of capsular collagen (blue arrowheads). AF, autofluorescence; TRITC, Texas red fluorescence filter.

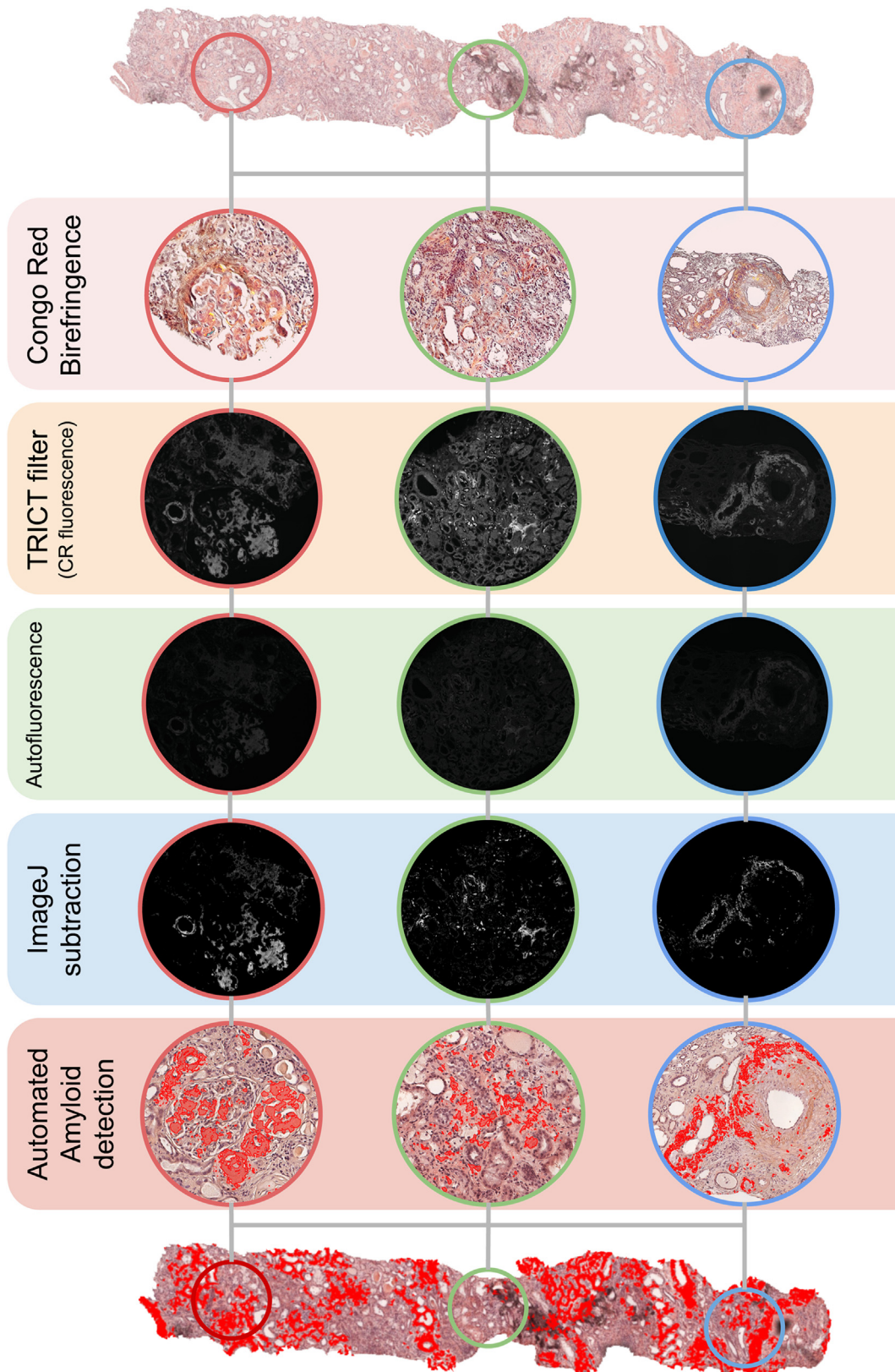


Figure 5.

Output of the automated image analysis pipeline (streamlined pipeline for amyloid detection through Congo Red [CR] fluorescence digital analysis) on an exemplificative case of renal biopsy with CR positivity within glomerular, vascular, and interstitial compartments. TRITC, Texas red fluorescence filter.

However, the assessment of positivity should be accompanied by a critical evaluation of the quality of the virtual slide, as out-of-focus areas and scan artifacts could affect the assessment,³² as shown by the misinterpretation of one of the cases as negative due to a scan artifact that was resolved after a rescan. With this in mind, it would be extremely important to have a method of objectively standardizing slide quality. By adopting standardized quality control measures, such as assessment of factors like staining intensity, background noise, and slide artifacts, laboratories could improve the accuracy and reliability of their diagnostic results.³³ Quantification and localization of deposits in different renal compartments provided valuable insights into the accuracy of both methods. Good interobserver agreement was observed throughout the AS, which was also reflected in the individual AS components, with poorer performance in distinguishing mesangial involvement from capillary glomerular involvement, likely due to the lack of a morphology substrate when assessing fluorescence. In general, higher AS values were obtained with CRFVs, as the positive material could be more clearly delineated in fluorescence than with glass slide BR, which was particularly evident in the interstitial compartment. This discrepancy can be explained by the known misleading BR of collagen in the interstitial compartment, especially in fibrotic areas, which may lead to a cautious underestimation of interstitial amyloid deposition with the standard BR.³⁴ To improve the detection of amyloid deposits, we applied a computational approach to the images that retains only amyloids, removing artifacts, background, and normal tissue. To detect even small deposits without creating artifacts, we set up a pipeline that increases the amyloid signal intensity compared to auto-fluorescence without significantly changing the values between pixels (SPADA). By using such a computational tool, it was possible, for example, to overcome the interfering BR of the collagen-containing renal structures (eg, interstitium and capsule), providing the pathologist with a “cleaned” image containing only regions affected by amyloid deposits. The SPADA algorithm not only provides the pathologist with an additional image for immediate diagnosis but also has a number of additional applications. The resulting binary image, which can be easily converted from the newly acquired image, holds several possibilities, especially with the integration of ImageJ and QuPath software (Fig. 5).³⁵ This has significant implications, as these annotations can potentially guide microdissection of tissue samples for subsequent mass spectrometry analysis, which is the current gold standard for amyloid typing after its detection with CR.³⁶ Another promising in situ proteomic technique that combines morphology with functional/molecular information is matrix-assisted laser desorption ionization mass spectrometry, which has already demonstrated its importance in the study of various glomerulonephritis,^{37,38} especially thanks to the recent introduction of instruments with high molecular and spatial resolution that allow a single-cell approach to renal biopsies.³⁹ This approach has already provided promising results in the automatic detection and typing of amyloid,¹⁶ but coupling it with the SPADA algorithm could further increase the robustness of this method and reduce interobserver variability that may affect pathologists’ manual annotations. Finally, transferring annotations from the binary image to CR slides with light microscopy may revolutionize the approach to AL diagnosis by further improving the detection of tiny deposits directly on the WSI and enabling a more robust quantification of deposits by generating an objective “amyloid renal burden” score, paving the way for the application of machine learning and artificial intelligence tools to further advance amyloid detection and characterization.⁴⁰ This

study represents a first step in validating the evaluation of CRF directly from the virtual slide and demonstrates its general reliability in the routine diagnostic setting of a second-level nephropathology center after appropriate quality control of scanning. The proposed computational pipeline (SPADA algorithm) can be easily used by users through the full ImageJ macro script available at <https://github.com/Gizmopath/Amyloid>. Its implementation will allow further integration with proteomics and artificial intelligence techniques, ultimately leading to a higher standard of care for the patient.

Author Contributions

G.C., M.M.B., and V.L. defined the study design. G.C., M.D.S., F.Mascadri, and M.M.B. performed the scanning of renal biopsy samples, managed the virtual slides, and processed the obtained data. G.C. and M.M.B. developed the image analysis pipeline for renal biopsies. F.P. and V.L. provided blind scoring of the biopsies. A.S. and M.R. critically revised the manuscript. A.S. provided mother-tongue English grammar revision. V.L., F.P., F.A., F.Mescia, F.F., G.G., and A.E. acquired the funding and provided administrative support. All authors were involved in writing the paper and provided final approval of the submitted and published versions.

Data Availability

The data that support the findings of this study are available from the corresponding author upon reasonable request. The full ImageJ macro script is available at <https://github.com/Gizmopath/Amyloid>.

Funding

The work has been funded by the European Union - Next Generation EU - NRRP M6C2 - Investment 2.1 Enhancement and strengthening of biomedical research in the National Health Service (DIPLOMAT—PNRR-MR1-2022-12375735). F.P. is involved in the project by the Italian Ministry of the University MUR Dipartimenti di Eccellenza 2023-2027 (l. 232/2016, art. 1, commi 314-337). V.L., F.A., F.M., and A.S. thank the Ministry of Health grant RF GR-2021-12374235 PROFOUND.

Declaration of Competing Interest

No conflicts of interest declared.

Ethics Approval and Consent to Participate

Approval was obtained from the local ethics committee (PNRR-MR1-2022-12375735; March 16, 2023), informed consents were collected.

References

- Wechalekar AD, Gillmore JD, Hawkins PN. Systemic amyloidosis. *Lancet*. 2016;387(10038):2641–2654.
- Gertz MA. Immunoglobulin light chain amyloidosis: 2022 update on diagnosis, prognosis, and treatment. *Am J Hematol*. 2022;97(6):818–829.
- Muchtar E, Dispenzieri A, Magen H, et al. Systemic amyloidosis from A (AA) to T (ATTR): a review. *J Intern Med*. 2021;289(3):268–292.

4. L'Imperio V, Cazzaniga G, Vergani B, Smith AJ, Alberici F, Pagni F. Monoclonal gammopathy of renal significance: a molecular middle earth between oncology, nephrology, and pathology. *Kidney Dis (Basel)*. 2022;8(6):446–457.
5. Yakupova EI, Bobyleva IG, Vikhlyantsev IM, Bobylev AG. Congo red and amyloids: history and relationship. *Biosci Rep*. 2019;39(1):BSR20181415. <https://doi.org/10.1042/BSR20181415>
6. Brigger D, Muckle RJ. Comparison of Sirius red and Congo red as stains for amyloid in animal tissues. *J Histochem Cytochem*. 1975;23(1):84–88.
7. Cooper JH. An evaluation of current methods for the diagnostic histochemistry of amyloid. *J Clin Pathol*. 1969;22(4):410–413.
8. L'Imperio V, Fabbri P, Ferrario F, et al. Monoclonal gammopathy of renal significance: systemic involvement by benign condition. *Kidney Int*. 2015;88(1):200–202.
9. Klatskin G. Nonspecific green birefringence in Congo red-stained tissues. *Am J Pathol*. 1969;56(1):1–13.
10. L'Imperio V, Brambilla V, Cazzaniga G, Ferrario F, Nebuloni M, Pagni F. Digital pathology for the routine diagnosis of renal diseases: a standard model. *J Nephrol*. 2021;34(3):681–688.
11. L'Imperio V, Casati G, Cazzaniga G, et al. Improvements in digital pathology equipment for renal biopsies: updating the standard model. *J Nephrol*. Published online February 14, 2023. <https://doi.org/10.1007/s40620-023-01568-1>
12. Marcus A, Sadimin E, Richardson M, Goodell L, Fyfe B. Fluorescence microscopy is superior to polarized microscopy for detecting amyloid deposits in Congo red-stained trephine bone marrow biopsy specimens. *Am J Clin Pathol*. 2012;138(4):590–593.
13. Clement CG, Truong LD. An evaluation of Congo red fluorescence for the diagnosis of amyloidosis. *Hum Pathol*. 2014;45(8):1766–1772.
14. Shehabeldin A, Hussey C, Aggad R, Truong L. Increased diagnostic specificity of Congo red stain for amyloid: the potential role of Texas red-filtered fluorescence microscopy. *Arch Pathol Lab Med*. 2023;147(8):907–915. <https://doi.org/10.5858/arpa.2021-0512-OA>
15. Baxi V, Edwards R, Montalto M, Saha S. Digital pathology and artificial intelligence in translational medicine and clinical practice. *Mod Pathol*. 2022;35(1):23–32.
16. Bindi G, Smith A, Oliveira G, et al. Spatial resolution of renal amyloid deposits through MALDI-MSI: a combined digital and molecular approach to monoclonal gammopathies. *J Clin Pathol*. Published online February 22, 2023. <https://doi.org/10.1136/jcp-2023-208790>
17. Wu H, L'Imperio V, Rossi M, Kapp ME, Pauksakon P. Differences between κ and λ light chain amyloidosis analyzed by a pathologic scoring system. *Am J Clin Pathol*. 2023;160(2):144–149. <https://doi.org/10.1093/ajcp/aqad017>
18. Rubinstein S, Cornell RF, Du L, et al. Novel pathologic scoring tools predict end-stage kidney disease in light chain (AL) amyloidosis. *Amyloid*. 2017;24(3):205–211.
19. Hoelbeek JJ, Kers J, Steenbergen EJ, Roelofs JJTH, Florquin S. Renal amyloidosis: validation of a proposed histological scoring system in an independent cohort. *Clin Kidney J*. 2020;14(3):855–862.
20. Schneider CA, Rasband WS, Eliceiri KW. NIH Image to ImageJ: 25 years of image analysis. *Nat Methods*. 2012;9(7):671–675.
21. Davies DR, Redfield MM, Scott CG, et al. A simple score to identify increased risk of transthyretin amyloid cardiomyopathy in heart failure with preserved ejection fraction. *JAMA Cardiol*. 2022;7(10):1036–1044.
22. Wisniewski B, Wechalekar A. Confirming the diagnosis of amyloidosis. *Acta Haematol*. 2020;143(4):312–321.
23. Pauksakon P, Revelo MP, Horn RG, Shappell S, Fogo AB. Monoclonal gammopathy: significance and possible causality in renal disease. *Am J Kidney Dis*. 2003;42(1):87–95.
24. Patel A, Balis UGJ, Cheng J, et al. Contemporary whole slide imaging devices and their applications within the modern pathology department: a selected hardware review. *J Pathol Inform*. 2021;12:50.
25. Howie AJ. Origins of a pervasive, erroneous idea: the “green birefringence” of Congo red-stained amyloid. *Int J Exp Pathol*. 2019;100(4):208–221.
26. El-Meanawy A, Mueller C, Iczkowski KA. Improving sensitivity of amyloid detection by Congo red stain by using polarizing microscope and avoiding pitfalls. *Diagn Pathol*. 2019;14(1):57.
27. Howie AJ, Owen-Casey MP. Systematic review of accuracy of reporting of Congo red-stained amyloid in 2010–2020 compared with earlier. *Ann Med*. 2022;54(1):2511–2516.
28. Cohen AS, Calkins E, Levene CI. Studies on experimental amyloidosis. I. Analysis of histology and staining reactions of casein-induced amyloidosis in the rabbit. *Am J Pathol*. 1959;35(5):971–989.
29. Giordadze TA, Shiina N, Baloch ZW, Tomaszewski JE, Gupta PK. Improved detection of amyloid in fat pad aspiration: an evaluation of Congo red stain by fluorescent microscopy. *Diagn Cytopathol*. 2004;31(5):300–306.
30. Linke RP. Highly sensitive diagnosis of amyloid and various amyloid syndromes using Congo red fluorescence. *Virchows Arch*. 2000;436(5):439–448.
31. Evans AJ, Brown RW, Bui MM, et al. Validating whole slide imaging systems for diagnostic purposes in pathology. *Arch Pathol Lab Med*. 2022;146(4):440–450.
32. Kumar N, Gupta R, Gupta S. Whole slide imaging (WSI) in pathology: current perspectives and future directions. *J Digit Imaging*. 2020;33(4):1034–1040.
33. Haghighat M, Browning L, Sirinukunwattana K, et al. Automated quality assessment of large digitised histology cohorts by artificial intelligence. *Sci Rep*. 2022;12(1):5002.
34. Khurana R, Uversky VN, Nielsen L, Fink AL. Is Congo red an amyloid-specific dye? *J Biol Chem*. 2001;276(25):22715–22721.
35. Bankhead P, Loughrey MB, Fernández JA, et al. QuPath: open source software for digital pathology image analysis. *Sci Rep*. 2017;7(1):16878.
36. Dasari S, Theis JD, Vrana JA, et al. Amyloid typing by mass spectrometry in clinical practice: a comprehensive review of 16,175 samples. *Mayo Clin Proc*. 2020;95(9):1852–1864.
37. L'Imperio V, Smith A, Chinello C, Pagni F, Magni F. Proteomics and glomerulonephritis: a complementary approach in renal pathology for the identification of chronic kidney disease related markers. *Proteomics Clin Appl*. 2016;10(4):371–383.
38. Smith A, L'Imperio V, Ajello E, et al. The putative role of MALDI-MSI in the study of membranous nephropathy. *Biochim Biophys Acta: Proteins Proteom*. 2017;1865(7):865–874.
39. Smith A, L'Imperio V, Denti V, et al. High spatial resolution MALDI-MS imaging in the study of membranous nephropathy. *Proteomics Clin Appl*. 2019;13(1):e1800016.
40. Allegra A, Mirabile G, Tonacci A, Genovese S, Pioggia G, Gangemi S. Machine learning approaches in diagnosis, prognosis and treatment selection of cardiac amyloidosis. *Int J Mol Sci*. 2023;24(6):5680. <https://doi.org/10.3390/ijms24065680>